Divalent Mercury in Dissolved Organic Matter Is Bioavailable to Fish and Accumulates as Dithiolate and Tetrathiolate Complexes

Jean-Paul Bourdineaud, Maria Gonzalez-Rey, Mauro Rovezzi, Pieter Glatzel, Kathryn Nagy, Alain Manceau

Divalent mercury in dissolved organic matter is bioavailable to fish and accumulates as dithiolate and tetrathiolate complexes

Jean-Paul Bourdineaud,*,† Maria Gonzalez-Rey,‡ Mauro Rovezzi,§ Pieter Glatzel,§ Kathryn L. Nagy,‖ Alain Manceau*,∞

†Institut Européen de Chimie et Biologie, Université de Bordeaux, CNRS, 2 rue Escarpit, 33607 Pessac, France

‡Laboratoire EPOC, Université de Bordeaux, CNRS, 33120 Arcachon, France.

§European Synchrotron Radiation Facility (ESRF), 71 Rue des Martyrs, 38000 Grenoble, France

‖Department of Earth and Environmental Sciences, University of Illinois at Chicago, MC-186, 845 West Taylor Street, Chicago, Illinois 60607, United States

∞ISTerre, Université Grenoble Alpes, CNRS, 38000 Grenoble, France

*Corresponding Authors :

E-mail: jean-paul.bourdineaud@u-bordeaux.fr

E-mail: alain.manceau@univ-grenoble-alpes.fr. Phone: +33 4 76 63 51 93.

Keywords: Mercury, fish, DOM, speciation, metacinnabar, XANES

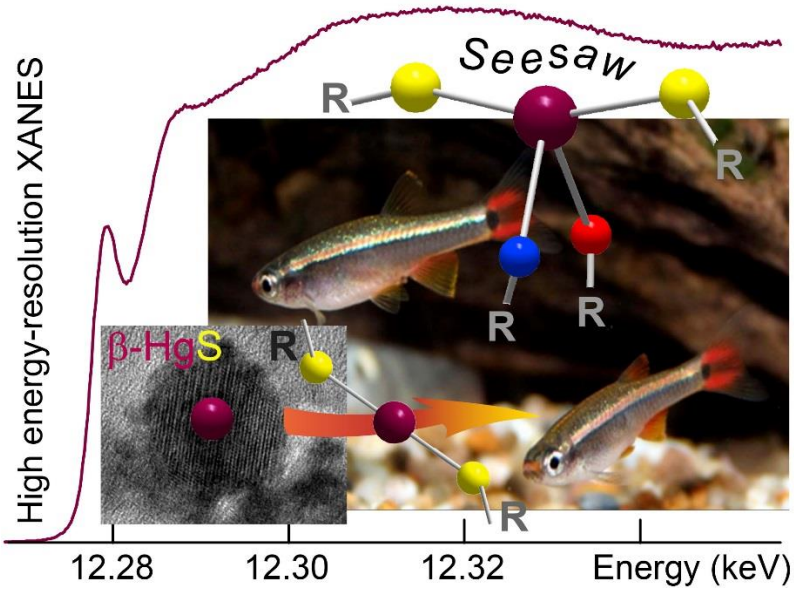

ABSTRACT

The freshwater cyprinid *Tanichthys albonubes* was used to assess the bioavailability of divalent mercury (Hg(II)) complexed in dissolved organic matter (DOM) to fish. The fish acquired 0.3 to 2.2 μg Hg/g dry weight after eight weeks in aquaria containing DOM from a *Carex* peat with complexed mercury at initial concentrations of 14 nM to 724 nM. Changes in the relative proportions of dithiolate $Hg(SR)_2$ and nanoparticulate β-HgS in the DOM, as quantified by high energy-resolution XANES (HR-XANES) spectroscopy, indicate that $Hg(SR)_2$ complexes either produced by microbially-induced dissolution of nanoparticulate β-HgS in the DOM or present in the original DOM were the forms of mercury that entered the fish. In the fish with 2.2 μg Hg/g, 84 ± 8% of Hg(II) was bonded to two axial thiolate ligands and one or two equatorial N/O electron donors ($Hg[(SR)_2+(N/O)_{1-2}]$ coordination), and 16% had a $Hg(SR)_4$ coordination, as determined by HR-XANES. For comparison, fish exposed to Hg^{2+} from 40 nM $HgCl_2$ contained 10.4 μg Hg/g in the forms of dithiolate (20 ± 10%) and tetrathiolate (23 ± 10%) complexes, and also Hg_xS_y clusters (57 ± 15%) having a β-HgS-type local structure and a dimension that exceeded the size of metallothionein clusters. There was no evidence of methylmercury in the fish or DOM within the 10% uncertainty of the HR-XANES. Together, the results indicate that inorganic Hg(II) bound to

DOM is a source of mercury to biota with dithiolate $Hg(SR)_2$ complexes as the immediate species bioavailable to fish, and that these complexes transform in response to cellular processes.

INTRODUCTION

Mercury (Hg) is a potent neurotoxin in animals and humans that bioaccumulates in aquatic food webs mainly as organic methylmercury (MeHg). Although dietary ingestion of MeHg is the primary exposure pathway in fish, exposure also occurs by intake of waterborne forms of MeHg and inorganic (Hg(II)) mercury, both of which can rapidly contaminate an entire ecosystem. Field and laboratory experiments showed that 10% to 38% of total mercury accumulated in fish can originate directly from water.[1-6] The relative importance of the food and water entryways may be seasonal, with a water source dominating in the spring and fall, for example reaching up to 80% of the total MeHg accumulated in yellow perch (*Perca flavescens*), and a food source dominating in the summer.[7] In previous experiments conducted with free ionic mercury species ($MeHg^+$, Hg^{2+}), mercury was considered to enter fish tissues through gills. However, mercury is strongly bound to dissolved organic matter (DOM) in aquatic systems,[8] and therefore may not be readily available for respiratory uptake. Mercury was less bioavailable to fish and zooplankton in the field and in laboratory experiments when complexed to DOM.[9-22] Similarly, complexation to DOM has also been shown to reduce the toxicity of Zn to rainbow trout[9] and the toxicity of both Zn and Cd to the microalga *Pseudokirchneriella subcapitata*.[23]

In contrast, other studies have reported that Hg concentration in fish increases with the amount of dissolved organic carbon (DOC).[13, 24-29] In aquatic invertebrates from Arctic tundra lakes, mercury bioaccumulation was promoted at [DOC] < 8.8 mg C/L, but inhibited above this concentration.[30] Bioaccumulation, toxicity, and uptake level of Cd by aquatic organisms all have been shown to increase in the presence of DOM in freshwater and seawater.[9, 31-33] Lastly, under

anaerobic conditions, *Desulfovibrio desulfuricans* bacteria were able to methylate Hg complexed to DOM,[34] indicating that at least some of the complexed Hg is easily bioavailable.

The molecular structure of any metal cation in the DOM must play a principal role in the processes that lead to bioavailability. Inorganic Hg in DOM occurs in two dominant forms: a linear dithiolate complex ($Hg(SR)_2$) and nanoparticulate metacinnabar (β-HgS_{NP}).[35-37] These forms may be altered under oxygenated biotic conditions, for example as a result of the microbial production of extracellular low-molecular-weight (LMW) thiols that might extract Hg from the larger molecules of DOM.[38]

The forms of inorganic Hg in DOM that are bioavailable to fish were assessed by exposing *Tanichthys albonubes*, which belongs to the Cyprinidae family like *Denio rerio* (zebrafish), to DOM pre-equilibrated with Hg(II) in aquaria. After eight weeks, the molecular structures of Hg in the DOM and fish were determined by high energy-resolution X-ray absorption near-edge structure (HR-XANES) spectroscopy.[37, 39] The initial concentration of DOM was fixed to 29.6 mg C/L, and the Hg concentration in the initial DOM was varied from 28 to 1453 μg Hg/g dry DOM producing 14 to 724 nM Hg(II) in the aquaria. For comparison, dissolved organic carbon (DOC) concentrations range from 10 to 80 mg/L in peatland pore waters from North America,[40] and from 60 to 200 mg/L in coastal lagoons in Rio de Janeiro State, Brazil.[41, 42] The mercury concentrations are representative of contaminated water, beginning just above the 10 nM maximum contaminant level (MCL) for inorganic mercury in primary drinking water. [43] Changes from the initial β-HgS_{NP}: $Hg(SR)_2$ ratio in the DOM and characterization of the molecular structure of mercury in the fish would indicate processes that may release Hg from the DOM, making it bioavailable. The forms of mercury in the fish potentially could be biomarkers of exposure to inorganic mercury sourced from DOM in aquatic systems.

MATERIALS AND METHODS

A detailed description of the experimental and computational methods is given in the Supporting Information (SI).

Preparation of Hg-DOM. The DOM was extracted from a *Carex* peat.[44, 45] Divalent mercury was added at pH 6 to obtain initial concentrations of 28, 270, and 1453 μg Hg/g dry DOM (hereafter called DOM_i-28, DOM_i-270 and DOM_i-1453), and the Hg-DOM solutions were aged in the dark for six months following the protocol described previously for Hg(II) complexed to Elliott Soil humic acid.[37]

Fish exposure to Hg(II)-DOM and dissolved $HgCl_2$. Fifty-five adult *T. albonubes* were placed in each of 12 separate aquaria containing aerated chlorine-free water at pH 7.7 ± 0.05 and maintained at 21 ± 4 °C, and six experimental conditions were replicated. Three were controls: C_0, without DOM and without Hg(II); C_{DOM}, with DOM and without Hg(II); and C_{Hg}, without DOM and with 8 μg/L Hg^{2+} (40 nM Hg) from a $HgCl_2$ stock solution (> 99.5% purity, Merck). For the other three, the stock Hg-DOM suspensions containing 570 mg DOM/L were diluted in the aquaria to a final concentration of 100 mg DOM/L, or 29.6 mg DOC/L yielding calculated initial Hg concentrations of 14 nM or 2.8 μg/L (DOM_i-28), 135 nM or 27 μg/L (DOM_i-270), and 724 nM or 145 μg/L (DOM_i-1453).[46] Total Hg concentrations were measured in water (n = 4, 2 per duplicated aquarium) at the start of the experiment (t_0) and after one (t_1), two (t_2), four (t_4), and eight (t_8) weeks (t_8) for all aquaria and in whole fish (n = 6, 3 per duplicated aquarium) at t_1, t_2 , t_4 and t_8 for all aquaria except C_0. Mercury concentration was determined in six fish at t_0 from the acclimatization tank. After eight weeks, whole fish from the DOM_i-1453 and C_{Hg} experiments were lyophilized and analyzed by HR-XANES spectroscopy. Freeze-drying a frozen tissue does not change the speciation of the metal.[47, 48] The possibility of methylation in the Hg-DOM experiments

was tested by comparison to a separate experiment in which fish were exposed to MeHg (C_{MeHg}), as described previously.[49]

Hg Analyses. Mercury in fish was quantified with an AMA-254 mercury analyzer (Altec, Prague) (fish) and in DOM with a DMA-80 (Milestone, Dual-Cell).

HR-XANES spectroscopy. Mercury L_3-edge HR-XANES spectra were measured at 10-15 K with high-reflectivity analyzer crystals[50] on beamline ID26 at the European Synchrotron Radiation Facility (ESRF). Data were analyzed against a large database of spectra for mercury minerals (α-HgS, β-HgS, β-HgS_{NP}), Hg(II) complexes in natural organic matter, and Hg(II) and methylmercury (MeHg) model complexes with thiolate ligands.[36, 37, 39, 51, 52] . All reference spectra were considered as a basis for identification, but only diagnostic spectra are discussed herein.

Geometry optimization of model Hg complexes. The geometries of structural models for the Hg complexes were optimized at a high level of molecular orbital theory (MP2/TZVP-ecp) using ORCA 3.0.3[53] and a computational scheme tested previously on the modeling of the structure and stability of monomeric Hg–thiolate complexes,[36, 37, 54] and herein on the $Hg(Cysteamine)_2$ complex (Figure S1).

RESULTS

Transfer of Hg(II) from DOM to fish. Chemical analyses of fish tissue show that Hg(II) initially bound to DOM became bioavailable (Table 1). Whole fish exposed to initial [Hg_{DOM}] of 2.8, 27, and 145 μg/L (14 to 724 nM) contained corresponding amounts of 0.33, 1.06, and 2.20 μg Hg/g dry weight fish after eight weeks. Fish in the control C_0 aquaria with neither Hg nor DOM contained 0.022 ± 0.007 μg Hg/g wet weight (0.09 ± 0.03 μg Hg/g dry weight). The amounts of mercury in the fish after eight weeks corrected for the amount in the control fish (C_0) were 1.9, 0.88, and 0.32 %, respectively, of the total final mass of Hg present in aquaria in both water and

fish. The fraction of Hg(II) transferred to fish was much higher in the C_{Hg} aquaria with initial [$HgCl_2$] of 8 μg/L (40 nM), reaching 50% after eight weeks (Table S1). Total Hg in whole fish exposed to Hg-DOM ranged from 3 to 21% of the amount in fish in the C_{Hg} experiment with $HgCl_2$ (10.4 μg Hg/g fish) and was 3 to 24 times higher than the amount in the control C_0 experiment. Although the transfer percentages in the Hg-DOM experiments are low, they confirm that this pool of mercury can become bioavailable.

A higher percentage of Hg was bioavailable from DOM that contained lower amounts of Hg (Table 1). Conservative values for bioconcentration factors (BCFs), defined as the ratio of the chemical concentration in the fish (on a wet weight basis) to the initial concentration in water, were 27 in the [Hg_{DOM}] = 2.8 μg/L experiment and decreased to 8.3 and 4.4 in the [Hg_{DOM}] = 27 and 145 μg/L experiments, respectively. These BCFs follow the expected ecotoxicological rule for pollutant uptake by organisms (Table S2).

After eight weeks, the concentration of Hg in the DOM decreased from 28 to 2 μg/g (DOM_i-28, DOM_f-2), 270 to 27 μg/g (DOM_i-270, DOM_f-27), and 1453 to 240 μg/g (DOM_i-1453, DOM_f-240) (Table 1). Given that the amounts of Hg acquired by the fish were relatively small compared to the system totals, these large changes resulted from both an increase in the quantity of DOM over time, from food addition and production of biogenic DOM in the aquaria, and from loss of the initial DOM and its associated Hg to the filtration apparatus (SI and Table S3). Neither change in the amount of DOM in the systems was quantified.

Changes in proportions of molecular structures of Hg in DOM. The initial β-HgS_{NP}:$Hg(SR)_2$ ratio in the [Hg_{DOM}] = 2.8 μg/L experiment (DOM_i-28) decreased considerably after eight weeks (DOM_f-2) (Figure 1a). The DOM_i-28 spectrum was modeled as a linear combination of 88% β-HgS_{NP} and 12% $Hg(SR)_2$ (± 8 at. %) compared to 37% β-HgS_{NP} and 63% $Hg(SR)_2$ (± 10 at. %) in DOM_f-2 (Figures 1b and 1c and Table S4). This result suggests that nanoparticulate β-

HgS in DOM_i-28 was the main source of the Hg that became bioavailable, and also that new $Hg(SR)_2$ complexes may have been generated from the β-HgS. To demonstrate that the shift in species proportions required the presence of living organisms, the DOM_i-28 stock solution was diluted to the same concentration as in the fish aquaria, and aged at ambient temperature in air-equilibrated water for eight weeks, in the presence or absence of light. Spectra for these samples were similar to each other and to that of the original DOM_i-28 (Figure S2a) showing that the change in β-HgS:$Hg(SR)_2$ ratio was related to the presence of the fish.

In contrast to DOM_f-2, the changes in the ratio of β-HgS_{NP} to $Hg(SR)_2$ were smaller in DOM_f-27 and DOM_f-240 compared to the initial values (Figure S3) despite the observation that fish accumulated three times (DOM_f-27) and seven times (DOM_f-240) as much Hg as in the DOM_f-2 experiment (Table 1). The smaller variations in these ratios are directly related to the lower proportions of Hg transferred to fish (0.88 and 0.32%, respectively, of the Hg at t_8).

Form of Hg in fish from Hg-DOM experiments. Fish from the DOM_i-1453 experiment were examined by HR-XANES because the concentration of Hg was above the detection limit of 0.5 μg Hg/g[39] (Table 1). The spectrum (Fish-DOM) is distinct from those of the initial (DOM_i-1453) and final (DOM_f-240) DOM samples, and from those of fish contaminated with MeHg (Fish-MeHg from the C_{MeHg} experiment) and Hg^{2+} (Fish-Hg from the C_{Hg} experiment) (Figures 2a and 2b). Also, the molecular structure of Hg in Fish-DOM is not a simple mixture of the structures in fish exposed to MeHg and $HgCl_2$ (Figure 2c).

The Fish-DOM spectrum was most similar to those for Hg(II) complexed to L-glutathione ($Hg(GSH)_2$, with GSH = γ-Glu-Cys-Gly) and to L-cysteine ($Hg(Cys)_2$) at pH 7.5 from the spectral database[36, 37, 39, 51] (Figure 3a). Two component fits of $Hg(GSH)_2$ or $Hg(Cys)_2$ with $Hg(Cys)_4$ decreased the fit residuals (NSS) (Figure 3b) and both fits match the normalized X-ray absorption to within about 2% (Figure 3c). The species proportions are 88% $Hg(GSH)_2$ + 12% $Hg(Cys)_4$ or

80% $Hg(Cys)_2$ + 20% $Hg(Cys)_4$ with uncertainties of ± 8 %. Therefore, on average about 84% of the Hg in fish is two-coordinate ($Hg(SR)_2$) and 16% is four-coordinate ($Hg(SR)_4$).

The molecular structure of Hg in the fish is discerned by considering how glutathione and cysteine bond to Hg according to geometry optimization by *ab initio* post-Hartree-Fock computations.[36, 54] In $Hg(GSH)_2$, Hg(II) is bonded approximately linearly to the cysteinyl sulfur atoms at 2.33 Å from the two γ-Glu-Cys-Gly peptides and surrounded in trans-equatorial position by a carboxyl oxygen from a Gly residue at 2.62 Å, the backbone carbonyl oxygen at 2.88 Å from the Gly-Cys peptide bond (Gly-NH-CO-Cys) of the same GSH molecule, and an amide group (-NH) at 3.01 Å from the second GSH molecule (Figure 4a and Video S1). The shorter Hg-O distance is well below the sum of the van der Waals radii of 3.07 Å for the Hg-O pair, whereas the longer Hg-O distance approaches it, and the Hg-N distance is close to the value of 3.10 Å for the Hg-N pair. The two O atoms are close enough to Hg to be considered secondary bonding interactions, but the N atom is not. The complex is a double-ring chelate with one ring of six members and the other seven. The coordination of Hg is $Hg[(SR)_2+O_2]$, and the geometry is disphenoidal, or seesaw (i.e., an octahedron without two cis-equatorial ligands).[55] The S-Hg-S angle is bent to 167.2° by the carboxyl oxygen (Figures 4a), which on the HR-XANES spectrum is seen as a decrease in the near-edge peak intensity (Figures S4 and S5a).

The structure of the $Hg(Cys)_2$ complex depends on pH, which changes the protonation of the amine groups. The structure ranges from a nearly linear $Hg(SR)_2$ coordination with weak Hg-OOC contacts at 3.06-3.15 Å at pH 3 ($Hg(SR)_2$ coordination) to a bis five-membered ring chelate ($Hg[5\text{-}S/N\text{-}ring]_2$) with Hg coordination of $Hg(SR+NH_2)_2$ and disphenoidal geometry, like when bonded to GSH, at pH 11.5 (Figure S4). However, it is unlikely that both amine groups deprotonate and fold simultaneously to form a double-ring chelate,[39, 55-57] and therefore at pH 7.5, near physiological conditions, the Hg coordination is most likely dominantly $Hg[(SR)_2 + NH_2]$. The

structure of $Hg(GSH)_2$, which is bent by a carboxyl oxygen, and the structure of $Hg(Cys)_2$, which is bent by an amine group, give nearly identical HR-XANES traces (Figure S5a). We conclude that Hg is bonded in the Fish-DOM dithiolate complex to two cysteinyl sulfur atoms and to one or two nucleophilic donors, such as amine and amide nitrogen and carboxyl and carbonyl oxygen. The dithiolate Hg coordination in fish is denoted $Hg[(SR)_2+(N/O)_{1-2}]$.

The $Hg(Cys)_4$ complex, synthesized at pH 11.9, has four thiolate ligands at 2.52 Å,[51] a distance ~0.17 Å longer than that in $Hg(Cys)_2$. In HR-XANES, the post-edge absorption shifts to lower energy because of the increase in bond length in agreement with the Natoli rule[58] and, the near-edge peak disappears because of the tetrahedral coordination. Both features occur in the Fish-DOM spectrum. Although β-HgS_{NP} also has four-coordinate Hg(II), and therefore these same spectral features, there is no modulation at 12300 eV and above in the Fish-DOM spectrum indicative of the Hg-Hg pairs in β-HgS_{NP} (Figures 1 and S2). Thus, $Hg(Cys)_4$, with coordination denoted $Hg(SR)_4$, is considered a good representation of the tetrahedral coordination of Hg in fish.

Form of Hg in fish from the $Hg(Cl)_2$ experiment. The Fish-Hg spectrum has features like those of β-HgS_{NP} including a bumpy profile at high energy indicative of Hg-Hg pairs (Figure S6a). Linear least-squares fits identified β-HgS_{NP} as the first component, $Hg(Cys)_4$ as the second and $Hg(Cys)_2$ at pH 7.5 as the third, immediately followed by $Hg(GSH)_2$ (Figure S6a). A two-component fit with 83% β-HgS_{NP} + 17% $Hg(Cys)_4$ decreased NSS by 35% compared to the β-HgS_{NP} fit, and a three-component fit with 57±15% β-HgS_{NP} + 23±10% $Hg(Cys)_4$ + 20±10% $Hg(Cys)_2$ pH 7.5 decreased NSS by an additional 51%. Replacing $Hg(Cys)_2$ with $Hg(GSH)_2$ reduced NSS by an additional 49%, confirming that the two model complexes are indistinguishable. Both three-component best-fit residuals are as low as 1% (Figure S6b).

Form of Hg in fish from the methylmercury experiment. The spectrum for MeHg complexed to L-cysteine at pH 7.5 provided the best match to the Fish-MeHg spectrum, as expected[59] (Figure S7a). HR-XANES spectra of the MeHgCys complex as a function of pH and corresponding geometry optimizations show that the amine group is folded at pH ≥ 4.5 to form an aminothiolate ring chelate as in $Hg(Cys)_2$, except that the complex is a mono-cysteinate ($MeHg(SR+NH_2)$ coordination) (Figures S4e and S7). In comparison, the spectrum of MeHg complexed to DOM (Nordic Aquatic fulvic acid: NAFA-MeHg) has a deeper near-edge minimum and is shifted to the right in the range 12282-12286 eV (Figure S7b). Like in the comparison of Fish-DOM and pH 3 $Hg(Cys)_2$ spectra (Figure S5a), and the evolution of the MeHgCys spectra with pH (Figure S4d), this shift results from the lack of secondary N/O ligands in NAFA-MeHg. Thus, secondary coordination to N/O ligands, which occurs in Fish-MeHg, offers a means to differentiate a dithiolate complex in living ($Hg[(SR)_2+(N/O)_{1-2}]$ coordination) and detrital ($Hg[(SR)_2$ coordination) organic matter.[51]

In the C_{MeHg} experiment, no differences were observed within experimental noise of the HR-XANES measurements between spectra from gills, brain, liver and muscle, indicating that the binding environment is MeHg(SR+N/O) in all tissues, and that no demethylation occurred during the 28 days of experiment, even in liver[60-65] (Figure S7c). Thus, lack of an intense near-edge peak in Fish-DOM and Fish-Hg is direct evidence that these fish did not contain detectable methylmercury, implying that little to no MeHg formed in the DOM or biofilms in the oxygenated aquaria.

DISCUSSION

Experimental parameters and the environment. The initial DOM concentrations in the experiments are characteristic of natural aquatic environments, and the initial Hg concentrations

represent environments contaminated with point sources of mercury. In natural waters away from point sources, the concentration of dissolved Hg is between 0.2 and 15 ng/L, and most often below 5 ng/L.[40, 66] The experimental Hg concentration ranged from 2.8 to 145 μg/L, starting just above 2 μg/L which is the MCL for Hg in primary drinking water. With these higher initial concentrations of Hg in the aquaria and the eight-week experimental duration, fish obtained enough Hg for HR-XANES spectral acquisition within a reasonable timeframe. For example, the good quality Fish-DOM spectrum was obtained in only 6 hours using high-reflectivity analyzer crystals[48] on fish that acquired 2.1 μg Hg/g (2.1 ppm Hg) in the DOM_i-1453 experiment.

The amounts of mercury in the fish from the Hg-DOM experiments (0.33 to 2.1 μg Hg/g), bracket the amount of about 1 μg/g observed in wild fish from impacted areas[66-68] that acquire mercury over much longer periods. Despite a higher Hg/C ratio in the Hg-DOM experiments (94 to 4900 μg Hg/g C) than is typical of the natural uncontaminated environment (0.006 to 0.5 μg Hg/g C calculated with the experimental concentration of DOC), the mass fractions of total Hg transferred to the fish are in excellent agreement with results of similar experiments performed with midge larvae in which the Hg concentration was 0.1 μg/L and Hg/C ratios (0.1 to 1 μg Hg/g C) overlapped the natural range. The mass fraction of total Hg transferred to fish was 21% in the $HgCl_2$ experiment and 0.33% to 2.1% in the Hg-DOM experiments. In experiments with *Chaoborus* larvae, uptake of inorganic Hg(II) and MeHg decreased from 20% without DOM to less than 1% (Hg(II)) and 5% (MeHg) with DOM.[17]

Source and transfer of Hg from DOM to fish. The reduction of β-HgS_{NP} from 88% to 37% and associated increase of $Hg(SR)_2$ from 12% to 63% in the DOM_i-28/DOM_f-2 samples (Figure 1) suggests that β-HgS_{NP} provided the Hg that became bioavailable to fish. However, because nanoparticulate β-HgS that had formed abiotically in DOM[37, 69] was not observed in the fish, the β-HgS_{NP} must have dissolved and been transferred to fish in another form, probably through

276 exchange of bisthiolate-bound Hg at the surface of the gill epithelium.

277 Although the solubility of crystalline β-HgS is low (K_{sp} of $10^{-36.8}$ for the reaction $HgS_{(s)} + H^+ =$
278 $Hg^{2+} + HS^-$ at 25°C)[70], the nanoparticulate β-HgS in the DOM would be less stable, or more soluble,
279 than larger crystals[71] due to excess surface free energy. During the initial aging of the Hg-DOM
280 solutions, the DOM molecules likely adsorbed to nascent particles and slowed their crystal
281 growth,[72-75] and/or prevented their aggregation.[84] However, microbial communities in observed
282 DOM-biofilm assemblages in the aquaria could have produced small organic molecules that
283 promoted dissolution of the β-HgS_{NP}. Periphytic phototrophic microorganisms, such as algae, can
284 increase the bioavailability of Hg in such biofilms through the exudation of low-molecular-weight
285 (LMW) thiols, including thioglycolic acid, cysteine, and glutathione,[38] which are known to
286 participate in ligand-promoted dissolution of metal sulfides including nanoparticulate phases.[76]
287 Graham et al.[77] observed that Hg was more available for methylation by anaerobic bacteria in the
288 presence of DOM when the solution was slightly supersaturated with respect to β-HgS, indicating
289 that dissolution of nanoparticulate β-HgS in such systems is possible. Under oxic conditions,
290 however, added Hg(II) was more bioavailable to a bioreporter bacterium after short pre-
291 equilibration times (≤ 3h) with DOM than when DOM was absent or when Hg(II) and DOM had
292 pre-reacted for 24 h.[78] A reaction time of 24 h would have been sufficient to form β-HgS_{NP},[37, 79]
293 especially in the Suwannee River DOM used in ref. [78] because it is as rich in reduced sulfur as
294 peat,[45] and in this case, nanoparticulate β-HgS may not have dissolved. Those results also suggest
295 that Hg(II) associated with smaller nutrient carbon-bearing molecules was able to enter the
296 bacterial cells.[78]

297 We suspect that $Hg(SR)_2$ moieties in the DOM probably were also a source of Hg to the fish,
298 because in the DOM_i-1453 experiment this species unambiguously declined in proportion relative
299 to β-HgS_{NP} after eight weeks in the aquaria (Figure S3). DOM naturally contains low molecular

300 weight molecules. For example, 36% of the mass of Suwannee River fulvic acids can pass through
301 a dialysis membrane of 100 to 500 Da molecular weight cutoff,[80] and aqueous peat extracts can
302 permeate through human skin and exert physiological effects.[81] Also, larger DOM molecules could
303 be rapidly broken down by the activity of microbial heterotrophic communities naturally present
304 in the skin and digestive tract of fish. Upon degradation, DOM could release bioavailable thiol-
305 bound Hg(II) macromolecules, as has been shown for other metals.[82, 83] DOM can interact with
306 cell membranes,[23] increasing their permeability to passive uptake of neutral chemical species. In
307 various freshwater organisms, DOM is taken up directly via epithelia,[84] and upon exposure to
308 dried DOM, several nonspecific organic transporters were induced in the nematode
309 *Caenorhabditis elegans*.[85] Once internalized, DOM can migrate to organs or organelles and
310 provoke stress response reactions such as lipid peroxidation,[86] biotransformation activities,[85]
311 and induction of chemical defense proteins such as Hsp70.[87]

312 No MeHg was observed by HR-XANES in either DOM or the fish after eight weeks, presumably
313 because of the oxygenated conditions prevailing in the aquaria and the low concentration of
314 sulfate (8 mg/L). Even in anaerobic conditions, elevated sulfate is necessary for net methylation
315 of mercury by sulfato-reducing microorganisms.[88]

316 **Binding environments of Hg in fish.** We conclude that the mercury entered the fish as a low
317 molecular weight molecule in a $Hg(SR)_2$ coordination structure derived either from the DOM or
318 from microbial exudates that dissolved β-HgS_{NP} in the DOM. Internally, this mercury was
319 transformed to other coordinating environments. In the fish exposed to Hg(II)-spiked DOM, the
320 dominant species (84 ± 8% of total Hg equal to 2.2 μg/g) is a dithiolate complex with
321 $Hg[(SR)_2+(N/O)_{1-2}]$ coordination. The minor species, formed with the remaining 16 ± 8% Hg, is a
322 tetrathiolate $Hg(SR)_4$ complex. The fish exposed to $HgCl_2$ (Fish-Hg), which contained 10.4 μg
323 Hg/g, has as its dominant species a third Hg_xS_y form of larger nuclearity (56 ± 15%), with the two

mononuclear complexes in similar lesser proportions (20-23 ± 10%). The coordination environment of Hg in the three species is discussed below with the goal of indicating possible internal biological pathways for the transformations.

The Hg[$(SR)_2$+$(N/O)_{1-2}$] coordination. Divalent mercury is bonded in the dithiolate complex to two cysteinyl sulfur atoms at ~2.35 Å and to one or two electron donors at 2.5-3.0 Å. The secondary bonds are nearly perpendicular to the RS-Hg-SR bond axis, and cause the RS-Hg-SR angle to bend more, the shorter the bonds.[39, 89] The geometry optimizations show that the disphenoidal configuration can be obtained with both N and O ligands of different functionalities and molecular conformations. Besides the Hg($(SR)_2$+O_2) coordination from $Hg(GSH)_2$ and the Hg(SR+NH_2)$_2$ coordination from $Hg(Cys)_2$, two intramolecular disphenoidal geometries, both consistent with the HR-XANES results, were modeled. The Hg(Cys+GlyCysGly) model (Figure S8a) features a tetracoordinate double chelate with the cysteinyl NH_2 group at 2.57 Å and the carbonyl oxygen of the cysteine residue from the tripeptide at 2.73 Å. The oxygen of this functional group is electron rich because of its lone pairs and the C=O π bond, both favoring a nucleophilic attack on the positive mercury center. The $Hg(GlyCysGly)_2$ model (Figure S8b) features a tetracoordinate complex with the two O-terminal carboxylic groups at 2.55 and 2.57 Å. Disphenoidal geometry also may occur intermolecularly with side chain amine and guanidyl NH (e.g. from arginine[39, 90, 91]) groups via protein folding and ligand docking.[92-94]

Natural population analysis (NPA[95, 96]) shows that the partial atomic charge, hence the nucleophilicity, of the O and N donors decreases in the following order: NH_2 (-0.9 e) > COO^- (-0.8 e) > C=O (-0.7 e) > NH (-0.6 e) (Figures S1, S4 and S8). Amine and carboxyl groups are more likely to bond Hg than an amide. Their higher binding strength is reflected in the geometry optimizations by shorter Hg-NH_2 and Hg-COO^- bond distances and smaller S-Hg-S angles. However, other factors are involved in the stability of a macromolecular complex, such as the

conformation of the chelate, inter- and intra-molecular packing forces and interactions of the metal with other moieties (e.g., hydrogen bonds). For example, in plants Hg is selectively bonded to the thiol peptide phytochelatin PC2 over GSH, although the GSH concentration largely exceeds the PC2 concentration in the cytosol.[97-101] PC2 is a GSH dimer with the amino acid sequence $(\gamma\text{-Glu-Cys})_2$-Gly. The strong affinity of Hg for PC2 is explained by the formation of a bis six-membered ring chelate $Hg[6\text{-S/O-ring}]_2$ with the thiolate sulfur and carbonyl oxygen atoms from each cysteine residue ($Hg(SR+O)_2$ coordination (Figure S9).[51] The peptide forms a scaffold for the Hg complex: the two thiolate donors bind Hg like crab claws and the Cys-γGlu-Cys molecular cage is stabilized by one hydrogen bond between an amide proton and a carbonyl oxygen (>NH…O=C<), as is customary for the secondary structure of proteins. The calculated Hg-O distances are 2.65 Å and 2.95 Å and the SR-Hg-SR bond angle 164.0°, compared to d(Hg-O) = 2.62 Å and 2.88 Å and an angle of 167.2° for $Hg(GSH)_2$. As a result, the $Hg(GSH)_2$ and Hg(PC2) complexes have similar HR-XANES spectra (Figure S5b).

In animal and bacterial cells, Hg(II) is most commonly bonded to the consensus CXXC motif (single-letter amino acid code, where X can be any amino acid) of metalloproteins with the $Hg[(SR)_2+(N/O)_{1-2}]$ coordination. Examples include metallochaperones and metal-transporting ATPases MerP,[102] MerA,[94] and Atx1 and Ccc2.[103, 104] Interestingly, the chain length of the XX sequence (X = Ser, Gly, Ala,…) from the highly conserved motif GMTCXXC found in metalloproteins[105] is close to the γGlu length from the CXC motif of PC2.[48, 51] Thus, the CXXC motif can cause a distortion from linearity in the same way as Hg(PC2), $Hg(Cys)_2$ and $Hg(GSH)_2$. For example, the S-Hg-S bond angle is 167° in Atx1.[103] We conclude that the $Hg(Cys)_2$ and $Hg(GSH)_2$ models used in our HR-XANES analysis are good representations of the secondary bonding environment of dithiolated Hg in fish, whether intermolecular or intramolecular. Despite uncertainty on its exact nature, for energetic reasons Hg is more likely bonded in a claw setting

CXXC site of a protein.

The $Hg(SR)_4$ coordination. A high Cys/Hg ratio and non-physiological alkaline pH are required to form the $Hg(SR)_4$ coordination to low-molecular-weight ligands.[54, 57, 106] With proteins, monomeric tetrathiolate coordination has been described only in Hg-substituted rubredoxins, which are iron-sulfur electron-transfer proteins in sulfur-metabolizing bacteria and archaea.[107-109] The rarity of this coordination may be explained by the thermodynamic preference for $Hg(SR)_3$ over $Hg(SR)_4$ coordination from pH 4.8 to 10.6 in biological systems when the thiols are structurally connected.[54] The trigonal Hg(II)-SR complex is observed for instance in MerR[110] and the Hah1 metallochaperone.[92] In Hg(Hah1), Hg is covalently bonded to three sulfur atoms at 2.3-2.5 Å and weakly bonded to a fourth at 2.8 Å. We did not find any evidence for the trigonal coordination in fish, as modeled in our database with $Hg(D\text{-}Pen)_3$[56] and $[NEt_4][Hg(SC_6H_{11})_3]$.[111]

Four-fold coordination with sulfur atoms occurs, however, in polynuclear structures with thiolate ligands in metallothioneins ($Hg_x(SR)_y$)[48, 112] or with sulfide ligands in β-HgS.[113] The second structure model was favored in recent studies on the binding of Hg(II) to *Escherichia coli* and *Bacillus subtilis* under aerobic conditions using EXAFS and XANES spectroscopy.[114, 115] The authors identified the $Hg(SR)_4$ coordination and inferred that particulate $\beta\text{-}HgS_{(s)}$ precipitated from the reaction of biogenic sulfide with $Hg(SR)_2$.

Here, we favor the metallothionein (MT) interpretation because if β-HgS nanoparticles existed they should have been detectable by high energy-resolution XANES at liquid helium temperature. Fish metallothioneins have two metal binding domains. The α domain can bind four Hg atoms in a Hg_4Cys_{11} cluster and the β domain three Hg atoms in a Hg_3Cys_9 Hg_3Cys_9 cluster (Figure 4b).[48, 116] In each cluster the $Hg(Cys)_4$ tetrahedra are connected through their apices with a β-HgS-type core structure (Figure 4c). Metallothionein nanoclusters with nuclearity of only three to four are vanishingly small compared for example to β-HgS nanocrystals of 3-5 nm in

396 diameter observed by HRTEM in natural organic matter.[37] An α-Hg_4Cys_{11} cluster has on average
397 2.5 Hg-Hg pairs at 4.1-4.4 Å and a β-Hg_3Cys_9 cluster only 2, compared to 12 in β-HgS.[113] Both
398 clusters lack any Hg-Hg pairs beyond 7 Å. Because of the structural disorder and reduced size of
399 a MT $Hg_x(SR)_y$ core, the same HR-XANES fine structures that are associated with Hg-Hg pairs as
400 seen in the β-HgS_{NP} reference are smeared together and cannot be distinguished. A
401 metallothionein HR-XANES spectrum with a polynuclear core has a bell-shaped top edge with no
402 distinct modulation of the absorption signal: it appears like the spectrum from the $Hg(Cys)_4$
403 reference, even though some Hg-Hg pairs are present.[48, 51]

404 *The Hg_xS_y coordination*. Based on XANES calculations,[117, 118] a β-Hg_xS_y cluster size of at least 1
405 nm is required to produce the Hg-Hg multiple scattering events at the origin of the fine structures
406 in the HR-XANES spectrum of Fish-Hg (Figure S6a). This minimum size corresponds to a
407 stoichiometry of β-Hg_7S_{16}, which exceeds the maximum nuclearity of Hg_4S_{11} for the MT clusters.
408 Therefore, the Hg_xS_y coordination of Fish-Hg is most likely from particulate β-HgS which could
409 form in the reducing environment of the cytosol by the reaction of $Hg(SR)_2$ with hydrogen
410 (mono)sulfide (H_2S/HS^-).[114, 115]

411 The absence of compelling evidence for nanoparticulate β-HgS in Fish-DOM can be explained,
412 at least in part, by the fact that fish from the DOM experiment had only 20% of the Hg that was in
413 fish from the $HgCl_2$ experiment. The dithiolate and tetrathiolate Hg species, which coexist in both
414 Fish-DOM and Fish-Hg, are probably more representative of the forms of inorganic Hg at
415 environmental concentrations. Lastly, although the same, or closely related, β-HgS-type
416 nanoparticles occur in DOM and in Fish-Hg, the DOM nanoparticles most likely transformed
417 externally to $Hg(SR)_2$ prior to mercury incorporation in fish tissue. Furthermore, the two mercury
418 sulfides formed by different reaction pathways. In Hg-DOM, the β-HgS nanocrystals were
419 produced under aerated conditions from $Hg(SR)_2$ by a dealkylation reaction,[37, 69] whereas in fish

the β-Hg_xS_y clusters were likely formed by reaction of $Hg(SR)_2$ with biogenic sulfide.[114, 115] Although most mercury in fish tissue is methylmercury,[66] the presence in fish of any of the structures observed in the Fish-DOM or Fish-Hg spectra would be a biomarker of an inorganic Hg source and may have potential for forensic applications.

ASSOCIATED CONTENT

Supporting Information

The Supporting Information is available free of charge on the ACS Publications website at DOI: Supplemental information on materials and methods, Supplementary Tables and Figures, Cartesian coordinates of the $Hg(Cys)_2$ and $Hg(GSH)_2$ complexes, $Hg_4(SMe)_{11}$-α and $Hg_3(SMe)_9$-β clusters, and HR-XANES spectra (PDF). Video S1 showing the structures of $Hg(GSH)_2$.

AUTHOR INFORMATION

Corresponding Authors

E-mail: jean-paul.bourdineaud@u-bordeaux.fr
E-mail: alain.manceau@univ-grenoble-alpes.fr

Notes

The authors declare no competing financial interests.

ACKNOWLEDGMENTS

Support was provided to A.M, M.G-R., K.L.N., and J-P.B. by the French National Research Agency (ANR) under grant ANR-12-BS06-0008-01, to A.M., M.R., and P.G. by the ANR under grant ANR-10-EQPX-27-01 (EcoX Equipex), and to K.L.N. by the U.S. National Science Foundation under grant EAR-1628956. The Froggy platform of the CIMENT infrastructure (ANR Grant ANR-10-EQPX- 29-01) provided computing resources and Pierre Girard his expertise in parallel scientific processing. Martine Lanson synthesized the Hg-DOM and performed Hg analyses with Aude Wack.

REFERENCES

(1) Phillips, G. R.; Buhler, D. R., The relative contributions of methylmercury from food or water to rainbow-trout (Salmo gairdneri) in a controlled laboratory environment. *Trans. Am. Fish. Soc.* **1978,** *107*, 853-861.

(2) Rodgers, D. W.; Qadri, S. U., Growth and mercury accumulation in yearling yellow perch, *Perca flavescens,* in the Ottawa River, Ontario. *Environ. Biol. Fish.* **1982,** *7*, 377-383.

(3) Meili, M., Fluxes, pools, and turnover of mercury in swedish forest lakes. *Water Air Soil Poll.* **1991,** *56*, 719-727.

(4) Spry, D. J.; Wiener, J. G., Metal bioavailability and toxicity to fish in low-alkalinity lakes - A critical review. *Environ. Pollut.* **1991,** *71*, 243-304.

(5) Hall, B. D.; Bodaly, R. A.; Fudge, R. J. P.; Rudd, J. W. M.; Rosenberg, D. M., Food as the dominant pathway of methylmercury uptake by fish. *Water Air Soil Poll.* **1997,** *100*, 13-24.

(6) Hrenchuk, L. E.; Blanchfield, P. J.; Paterson, M. J.; Hintelmann, H. H., Dietary and waterborne mercury accumulation by yellow perch: A field experiment. *Environ. Sci. Technol.* **2012,** *46*, 509-516.

(7) Post, J. R.; Vandenbos, R.; McQueen, D. J., Uptake rates of food-chain and waterborne mercury by fish: Field measurements, a mechanistic model, and an assessment of uncertainties. *Can. J. Fish. Aquat. Sci.* **1996,** *53*, 395-407.

(8) Haitzer, M.; Aiken, G. R.; Ryan, J. N., Binding of mercury(II) to dissolved organic matter: The role of the mercury-to-DOM concentration ratio. *Environ. Sci. Technol.* **2002,** *36*, 3564-3570.

(9) Ramamoorthy, S.; Blumhagen, K., Uptake of Zn, Cd, and Hg by fish in the presence of competing compartments. *Can. J. Fish. Aquat. Sci.* **1984,** *41*, 750-756.

(10) Grieb, T. M.; Driscoll, C. T.; Gloss, S. P.; Schofield, C. L.; Bowie, G. L.; Porcella, D. B., Factors affecting mercury accumulation in fish in the Upper Michigan peninsula. *Environ. Toxicol. Chem.* **1990,** *9*, 919-930.

(11) Playle, R. C.; Dixon, D. G.; Burnison, K., Copper and cadmium-binding to fish gills - Modification by dissolved organic-carbon and synthetic ligands. *Can. J. Fish. Aquat. Sci.* **1993,** *50*, 2667-2677.

(12) Back, R. C.; Watras, C. J., Mercury in zooplankton of northern Wisconsin lakes - Taxonomic and site-specific trends. *Water Air and Soil Poll.* **1995,** *80*, 931-938.

(13) Driscoll, C. T.; Blette, V.; Yan, C.; Schofield, C. L.; Munson, R.; Holsapple, J., The role of dissolved organic carbon in the chemistry and bioavailability of mercury in remote Adirondack lakes. *Water Air and Soil Poll.* **1995,** *80*, 499-508.

(14) Hollis, L.; Muench, L.; Playle, R. C., Influence of dissolved organic matter on copper binding, and calcium on cadmium binding, by gills of rainbow trout. *J. Fish Biol.* **1997,** *50*, 703-720.

(15) Penttinen, S.; Kostamo, A.; Kukkonen, J. V. K., Combined effects of dissolved organic material and water hardness on toxicity of cadmium to *Daphnia magna*. *Environ. Toxicol. Chem.* **1998,** *17*, 2498-2503.

(16) Richards, J. G.; Burnison, B. K.; Playle, R. C., Natural and commercial dissolved organic matter protects against the physiological effects of a combined cadmium and copper exposure on rainbow trout (*Oncorhynchus mykiss*). *Can. J. Fish. Aquat. Sci.* **1999,** *56*, 407-418.

(17) Sjoblom, A.; Meili, M.; Sundbom, M., The influence of humic substances on the speciation and bioavailability of dissolved mercury and methylmercury, measured as uptake by *Chaoborus* larvae and loss by volatilization. *Sci. Tot. Environ.* **2000,** *261*, 115-124.

(18) Richards, J. G.; Curtis, P. J.; Burnison, B. K.; Playle, R. C., Effects of natural organic matter source on reducing metal toxicity to rainbow trout (*Oncorhynchus mykiss*) and on metal binding to their gills. *Environ. Tox. Chem.* **2001,** *20*, 1159-1166.

(19) Meinelt, T.; Playle, R. C.; Pietrock, M.; Burnison, B. K.; Wienke, A.; Steinberg, C. E. W., Interaction of cadmium toxicity in embryos and larvae of zebrafish (*Danio rerio*) with calcium and humic substances. *Aquat. Toxicol.* **2001,** *54*, 205-215.

(20) Van Ginneken, L.; Bervoets, L.; Blust, R., Bioavailability of Cd to the common carp, *Cyprinus carpio*, in the presence of humic acid. *Aquat. Toxicol.* **2001,** *52*, 13-27.

(21) Hammock, D.; Huang, C. C.; Mort, G.; Swinehart, J. H., The effect of humic acid on the uptake of mercury(II), cadmium(II), and zinc(II) by Chinook salmon (*Oncorhynchus tshawytscha*) eggs. *Arch. Environ. Con. Tox.* **2003,** *44*, 83-88.

(22) Burnison, B. K.; Meinelt, T.; Playle, R.; Pietrock, M.; Wienke, A.; Steinberg, C. E. W., Cadmium accumulation in zebrafish (*Danio rerio*) eggs is modulated by dissolved organic matter (DOM). *Aquat. Toxicol.* **2006,** *79*, 185-191.

(23) Koukal, B.; Gueguen, C.; Pardos, M.; Dominik, J., Influence of humic substances on the toxic effects of cadmium and zinc to the green alga *Pseudokirchneriella subcapitata*. *Chemosphere* **2003,** *53*, (8), 953-961.

(24) Mannio, J.; Verta, M.; P., K.; Rekolainen, S., The effect of water quality on the mercury concentration of northern pike (*Esox lucius* L.) in Finnish forest lakes and reservoirs. *Water Res. Inst. National Board of Waters, Helsinki, Pub.* **1986,** *65*, 32-43.

(25) McMurtry, M. J.; Wales, D. L.; Scheider, W. A.; Beggs, G. L.; Dimond, P. E., Relationship of mercury concentrations in lake trout (*Salvelinus namaycush*) and smallmouth bass (*Micropterus dolomieui*) to the physical and chemical characteristics of Ontario lakes. *Can. J. Fish. Aquat. Sci.* **1989,** *46*, 426-434.

(26) Hakanson, L.; Andersson, T.; Nilsson, A., Mercury in fish in Swedish lakes - Linkages to domestic and European sources of emission. *Water Air Soil Poll.* **1990,** *50*, 171-191.

(27) Wren, C. D.; Scheider, W. A.; Wales, D. L.; Muncaster, B. W.; Gray, I. M., Relation between mercury concentrations in walleye (*Stizostedion vitreum vitreum*) and northern pike (*Esox lucius*) in Ontario lakes and influence of environmental factors. *Can. J. Fish Aquat. Sci.* **1991,** *48*, 132-139.

(28) Penttinen, S.; Kukkonen, J.; Oikari, A., The kinetics of cadmium in *Daphnia magna* as affected by humic substances and water hardness. *Ecotox. Environ. Safe.* **1995,** *30*, 72-76.

(29) Watras, C. J.; Back, R. C.; Halvorsen, S.; Hudson, R. J. M.; Morrison, K. A.; Wente, S. P., Bioaccumulation of mercury in pelagic freshwater food webs. *Sci. Tot. Environ.* **1998,** *219*, 183-208.

(30) French, T. D.; Houben, A. J.; Desforges, J. P. W.; Kimpe, L. E.; Kokelj, S. V.; Poulain, A. J.; Smol, J. P.; Wang, X. W.; Blais, J. M., Dissolved organic carbon thresholds affect mercury bioaccumulation in Arctic lakes. *Environ. Sci. Technol.* **2014,** *48*, 3162-3168.

(31) Winner, R. W., The toxicity and bioaccumulation of cadmium and copper as affected by humic-acid. *Aquat. Toxicol.* **1984,** *5*, 267-274.

(32) Oikari, A.; Kukkonen, J.; Virtanen, V., Acute toxicity of chemicals to *Daphnia magna* in humic waters. *Sci. Tot. Environ.* **1992,** *118*, 367-377.

(33) Kozuch, J.; Pempkowiak, J., Molecular weight of humic acids as a major property of the substances influencing the accumulation rate of cadmium by a blue mussel (*Mytilus edulis*). *Environ. Int.* **1996,** *22*, 585-589.

(34) Graham, A. M.; Aiken, G. R.; Gilmour, C. C., Dissolved organic matter enhances microbial mercury methylation under sulfidic conditions. *Environ. Sci. Technol.* **2012,** *46*, 2715-2723.

(35) Skyllberg, U.; Bloom, P. R.; Qian, J.; Lin, C. M.; Bleam, W. F., Complexation of mercury(II) in soil organic matter: EXAFS evidence for linear two-coordination with reduced sulfur groups. *Environ. Sci. Technol.* **2006,** *40*, 4174-4180.

(36) Manceau, A.; Lemouchi, C.; Rovezzi, M.; Lanson, M.; Glatzel, P.; Nagy, K. L.; Gautier-Luneau, I.; Joly, Y.; Enescu, M., Structure, bonding, and stability of mercury complexes with thiolate and

thioether ligands from high-resolution XANES spectroscopy and first-principles calculations. *Inorg. Chem.* **2015,** *54*, 11776−11791.

(37) Manceau, A.; Lemouchi, C.; Enescu, M.; Gaillot, A.-C.; Lanson, M.; Magnin, V.; Glatzel, P.; Poulin, B. A.; Ryan, J. N.; Aiken, G. R.; Gautier-Luneau, I.; Nagy, K. L., Formation of mercury sulfide from Hg(II)-thiolate complexes in natural organic matter. *Environ. Sci. Technol.* **2015,** *49*, 9787−9796.

(38) Leclerc, M.; Planas, D.; Amyot, M., Relationship between extracellular low-molecular-weight thiols and mercury species in natural lake periphytic biofilms. *Environ. Sci. Technol.* **2015,** *49*, 7709−7716.

(39) Manceau, A.; Enescu, M.; Simionovici, A.; Lanson, M.; Gonzalez-Rey, M.; Rovezzi, M.; Tucoulou, R.; Glatzel, P.; Nagy, K. L.; Bourdineaud, J.-P., Chemical forms of mercury in human hair reveal sources of exposure. *Environ. Sci. Technol.* **2016,** *50*, 10721−10729.

(40) Mitchell, C. P. J.; Branfireun, B. A.; Kolka, R. K., Spatial characteristics of net methylmercury production hot spots in peatlands. *Environ. Sci. Technol.* **2008,** *42*, 1010-1016.

(41) Suhett, A. L.; Amado, A. M.; Enrich-Prast, A.; de Assis Esteves, F.; Farjalla, V. F., Seasonal changes of dissolved organic carbon photo-oxidation rates in a tropical humic lagoon: the role of rainfall as a major regulator. *Can. J. Fish. Aquat. Sci.* **2007,** *64*, 1266-1272.

(42) Suhett, A. L.; Amado, A. M.; Meirelles-Pereira, F.; Scofield, V.; Jacques, S. M. d. S.; Laque, T.; Farjalla, V. F., Origin, concentration, availability and fate of dissolved organic carbon in coastal lagoons of the Rio de Janeiro State. *Acta Limn. Brasil.* **2013,** *25*, 326-340.

(43) U.S. National Archives and Records Administration. 2018. Code of federal regulations. Title 40. Protection of Environment, Part 14. National Primary Drinking Water Regulations.

(44) Manceau, A.; Matynia, A., The nature of Cu bonding to natural organic matter. *Geochim. Cosmochim. Acta* **2010,** *74*, 2556-2580.

(45) Manceau, A.; Nagy, K. L., Quantitative analysis of sulfur functional groups in natural organic matter by XANES spectroscopy. *Geochim. Cosmochim. Acta* **2012,** *99*, 206-223.

(46) NIH, Guidelines for use of zebrafish in the NIH intramural research program. *http://oacu.od.nih.gov/ARAC/documents/Zebrafish.pdf* **2013**.

(47) George, G. N.; Pickering, I. J.; Pushie, M. J.; Nienaber, K.; Hackett, M. J.; Ascone, I.; Hedman, B.; Hodgson, K. O.; Aitken, J. B.; Levina, A.; Glover, C.; Lay, P. A., X-ray-induced photo-chemistry and X-ray absorption spectroscopy of biological samples. *J. Synch. Rad.* **2012,** *19*, 875-886.

(48) Manceau, A.; Bustamante, P.; Haouz, A.; Bourdineaud, J. P.; Gonzalez-Rey, M.; Geertsen, V.; Barruet, E.; Rovezzi, M.; Glatzel, P.; Pin, S., Mercury(II) binding to metallothionein in *Mytilus edulis* revealed by high energy-resolution XANES spectroscopy. *Chemistry - A European Journal* **2018**, doi.org/10.1002/chem.201804209.

(49) Gonzalez, P.; Dominique, Y.; Massabuau, J. C.; Boudou, A.; Bourdineaud, J. P., Comparative effects of dietary methylmercury on gene expression in liver, skeletal muscle, and brain of the zebrafish (*Danio rerio*). *Environ. Sci. Technol.* **2005,** *39*, 3972-3980.

(50) Rovezzi, M.; Lapras, C.; Manceau, A.; Glatzel, P.; Verbeni, R., High energy-resolution x-ray spectroscopy at ultra-high dilution with spherically bent crystal analyzers of 0.5 m radius. *Rev. Sci. Instr.* **2017,** *88*, 013108.

(51) Manceau, A.; Wang, J.; Rovezzi, M.; Glatzel, P.; Feng, X., Biogenesis of mercury-sulfur nanoparticles in plant leaves from atmospheric gaseous mercury. *Environ. Sci. Technol.* **2018,** *52*, 3935-3948.

(52) Lannes, A.; Manceau, A.; Rovezzi, M.; Glatzel, P.; Joly, Y.; Gautier-Luneau, I., Intramolecular Hg...π interactions of d-character with non-bridging atoms in mercury-aryl complexes. *Dalton Trans.* **2016,** *45*, 14035-14038.

(53) Neese, F., The ORCA program system. *WIREs Comput. Mol. Sci.* **2011,** *2*, 73-78.

(54) Enescu, M.; Manceau, A., High-level ab initio calculation of the stability of mercury–thiolate complexes. *Theor. Chem. Acc.* **2014,** *133*, n° 1457.

(55) Fleischer, H.; Dienes, Y.; Mathiasch, B.; Schmitt, V.; Schollmeyer, D., Cysteamine and its homoleptic complexes with group 12 metal ions. Differences in the coordination chemistry of Zn-^{II}, Cd-^{II}, and Hg-^{II} with a small N,S-donor ligand. *Inorg. Chem.* **2005,** *44*, 8087-8096.

(56) Leung, B. O.; Jalilehvand, F.; Mah, V., Mercury(II) penicillamine complex formation in alkaline aqueous solution. *Dalton Trans.* **2007**, 4666-4674.

(57) Warner, T.; Jalilehvand, F., Formation of Hg(II) tetrathiolate complexes with cysteine at neutral pH. *Can. J. Chem.* **2016,** *94*, 1–7.

(58) Bianconi, A.; Dell'Ariccia, M.; Gargano, A.; Natoli, C. R., Bond length determination using XANES. In *EXAFS and Near Edge Structure*, Bianconi, A.; Incoccia, A.; Stipcich, S., Eds. Springer, Berlin: 1983; Vol. 27, pp 57–61.

(59) Harris, H. H.; Pickering, I. J.; G.N., G., The chemical form of mercury in fish. *Science* **2003,** *301*, 1203.

(60) Arai, T.; Ikemoto, T.; Hokura, A.; Terada, Y.; Kunito, T.; Tanabe, S.; Nakai, I., Chemical forms of mercury and cadmium accumulated in marine mammals and seabirds as determined by XAFS analysis. *Environ. Sci. Technol.* **2004,** *38*, 6468-6474.

(61) Ikemoto, T.; Kunito, T.; Tanaka, H.; Baba, N.; Miyazaki, N.; Tanabe, S., Detoxification mechanism of heavy metals in marine mammals and seabirds: Interaction of selenium with mercury, silver, copper, zinc, and cadmium in liver. *Arch. Environ. Con. Tox.* **2004,** *47*, 402-413.

(62) Endo, T.; Kimura, O.; Hisamichi, Y.; Minoshima, Y.; Haraguchi, K.; Kakumoto, C.; Kobayashi, M., Distribution of total mercury, methyl mercury and selenium in pod of killer whales (Orcinus Orca) stranded in the northern area of Japan: Comparison of mature females with calves. *Environ. Poll.* **2006,** *144*, 145-150.

(63) Huggins, F. E.; Raverty, S. A.; Nielsen, O. S.; Sharp, N. E.; Robertson, J. D.; Ralston, N. V. C., An XAFS investigation of mercury and selenium in Beluga whale tissues. *Environ. Bioindic.* **2009,** *4*, 291-302.

(64) Nakazawa, E.; Ikemoto, T.; Hokura, A.; Terada, Y.; Kunito, T.; Tanabe, S.; Nakai, I., The presence of mercury selenide in various tissues of the striped dolphin: evidence from mu-XRF-XRD and XAFS analyses. *Metallomics* **2011,** *3*, 719-725.

(65) Lyytikainen, M.; Patynen, J.; Hyvarinen, H.; Sipila, T.; Kunnasranta, M., Mercury and selenium balance in endangered saimaa ringed seal depend on age and sex. *Environ. Sci. Technol.* **2015,** *49*, 11808-11816.

(66) Nevado, J. J. B.; Martin-Doimeadios, R. C. R.; Bernardo, F. J. G.; Moreno, M. J.; Herculano, A. M.; do Nascimento, J. L. M.; Crespo-Lopez, M. E., Mercury in the Tapajos River basin, Brazilian Amazon: A review. *Environ. Int.* **2010,** *36*, 593-608.

(67) Mathews, T. J.; Southworth, G.; Peterson, M. J.; Roy, W. K.; Ketelle, R. H.; Valentine, C.; Gregory, S., Decreasing aqueous mercury concentrations to meet the water quality criterion in fish: Examining the water-fish relationship in two point-source contaminated streams. *Sci. Tot. Environ.* **2013,** *443*, 836-843.

(68) Bourdineaud, J. P.; Durrieu, G.; Sarrazin, S. L. F.; da Silva, W. C. R.; Mourao, R. H. V.; de Oliveira, R. B., Mercurial exposure of residents of Santarem and Oriximina cities (Para, Brazil) through fish consumption. *Environ. Sci. Pollut. Res.* **2015,** *22*, 12150-12161.

(69) Enescu, M.; Nagy, K. L.; Manceau, A., Nucleation of mercury sulfide by dealkylation. *Sci. Rep.* **2016,** *6*, 39359.

635 (70) Drott, A.; Björn, E.; Boucher, S.; Skyllberg, U., Refining thermodynamic constants for
636 mercury(II)-sulfides in equilibrium with metacinnabar at sub-micromolar aqueous sulfide
637 concentrations. *Environ. Sci. Technol.* **2013,** *47*, 4197-4203.
638 (71) Liu, J.; Aruguete, D. M.; Murayama, M.; Hochella, M. F., Influence of size and aggregation on
639 the reactivity of an environmentally and industrially relevant nanomaterial (PbS). *Environ. Sci.*
640 *Technol.* **2009,** *43*, 8178-8183.
641 (72) Ravichandran, R.; Aiken, G. R.; Ryan, J. N.; Reddy, M. M., Inhibition of precipitation and
642 aggregation of metacinnabar (mercuric sulfide) by dissolved organic matter isolated from the
643 Florida Everglades. *Environ. Sci. Technol.* **1999,** *33*, 1418-1423.
644 (73) Gerbig, C. A.; Kim, C. S.; Stegemeier, J. P.; Ryan, J. N.; Aiken, G. R., Formation of nanocolloidal
645 metacinnabar in mercury-DOM-sulfide systems. *Environ. Sci. Technol.* **2011,** *45*, 9180-9187.
646 (74) Deonarine, A.; Hsu-Kim, H., Precipitation of mercuric sulfide nanoparticles in NOM-
647 containing water: Implications for the natural environment. *Environ. Sci. Technol.* **2009,** *43*, 2368–
648 2373.
649 (75) Slowey, A. J., Rate of formation and dissolution of mercury sulfide nanoparticles: The dual
650 role of natural organic matter. *Geochim. Cosmochim. Acta* **2010,** *74*, 4693–4708.
651 (76) Marchioni, M.; Gallon, T.; Worms, I.; Jouneau, P. H.; Lebrun, C.; Veronesi, G.; Truffier-Boutry,
652 D.; Mintz, E.; Delangle, P.; Deniaud, A.; Michaud-Soret, I., Insights into polythiol-assisted AgNP
653 dissolution induced by bio-relevant molecules. *Environ. Sci. Nano* **2018,** *5*, 1911-1920.
654 (77) Graham, A. M.; Aiken, G. R.; Gilmour, C. C., Effect of dissolved organic matter source and
655 character on microbial Hg methylation in Hg-S-DOM solutions. *Environ. Sci. Technol.* **2013,** *47*,
656 5746-5754.
657 (78) Chiasson-Gould, S. A.; Blais, J. M.; Poulain, A. J., Dissolved organic matter kinetically controls
658 mercury bioavailability to bacteria. *Environ. Sci. Technol.* **2014,** *48*, 3153-3161.
659 (79) Nagy, K. L.; Manceau, A.; Gasper, J. D.; Ryan, J. N.; Aiken, G. R., Metallothionein-like
660 multinuclear clusters of mercury(II) and sulfur in peat. *Environ. Sci. Technol.* **2011,** *45*, 7298–
661 7306.
662 (80) Remucal, C. K.; Cory, R. M.; Sander, M.; McNeill, K., Low molecular weight components in an
663 aquatic humic substance as characterized by membrane dialysis and orbitrap mass spectrometry.
664 *Environ. Sci. Technol.* **2012,** *46*, 9350-9359.
665 (81) Beer, A. M.; Junginger, H. E.; Lukanov, J.; Sagorchev, P., Evaluation of the permeation of peat
666 substances through human skin in vitro. *Int. J. Pharm.* **2003,** *253*, 169-175.

(82) Masson, M.; Blanc, G.; Schafer, J.; Parlanti, E.; Le Coustumer, P., Copper addition by organic matter degradation in the freshwater reaches of a turbid estuary. *Sci. Tot. Environ.* **2011,** *409*, 1539-1549.

(83) Wengel, M.; Kothe, E.; Schmidt, C. M.; Heide, K.; Gleixner, G., Degradation of organic matter from black shales and charcoal by the wood-rotting fungus *Schizophyllum commune* and release of DOC and heavy metals in the aqueous phase. *Sci. Tot. Environ.* **2006,** *367*, 383-393.

(84) Steinberg, C. E. W.; Meinelt, T.; Timofeyev, M. A.; Bittner, M.; Menzel, R., Humic substances. *Environ. Sci. Pollut. Res.* **2008,** *15*, 128-135.

(85) Menzel, R.; Sturzenbaum, S.; Barenwaldt, A.; Kulas, J.; Steinberg, C. E. W., Humic material induces behavioral and global transcriptional responses in the nematode *Caenorhabditis elegans*. *Environ. Sci. Technol.* **2005,** *39*, 8324-8332.

(86) Timofeyev, M. A.; Shatilina, Z. M.; Kolesnichenko, A. V.; Bedulina, D. S.; Kolesnichenko, V. V.; Pflugmacher, S.; Steinberg, C. E. W., Natural organic matter (NOM) induces oxidative stress in freshwater amphipods *Gammarus lacustris* Sars and *Gammarus tigrinus* (Sexton). *Sci. Tot. Environ.* **2006,** *366*, 673-681.

(87) Timofeyev, M. A.; Wiegand, C.; Burnison, B. K.; Shatilina, Z. M.; Pflugmacher, S.; Steinberg, C. E. W., Direct impact of natural organic matter (NOM) on freshwater amphipods. . *Sci. Total Environ.* **2004,** *319*, 115-121.

(88) Zhang, T.; Kucharzyk, K. H.; Kim, B.; Deshusses, M. A.; Hsu-Kim, H., Net methylation of mercury in estuarine sediment microcosms amended with dissolved, nanoparticulate, and microparticulate mercuric sulfides. *Environ. Sci. Technol.* **2014,** *48*, 9133-9141.

(89) Manceau, A.; Nagy, K. L., Relationships between Hg(II)-S bond distance and Hg(II) coordination in thiolates. *Dalton Trans.* **2008,** *11*, 1421-1425.

(90) Ratilla, E. M. A.; Kostic, N. M., Guanidyl groups - New metal-binding ligands in biomolecules - Reactions of chloro(2,2'.6',2"-terpyridine)platinum(II) with arginine in 2 cytochromes C and with other guanidyl ligands. *J. Am.. Chem. Soc.* **1988,** *110*, 4427-4428.

(91) Ratilla, E. M. A.; Scott, B. K.; Moxness, M. S.; Kostic, N. M., Terminal and new bridging coordination of methylguanidine, arginine, and canavanine to platinum(II) - The 1st crystallographic study of bonding between a transition-metal and a guanidine ligand. *Inorg. Chem.* **1990,** *29*, 918-926.

(92) Wernimont, A. K.; Huffman, D. L.; Lamb, A. L.; O'Halloran, T. V.; Rosenzweig, A. C., Structural basis for copper transfer by the metallochaperone for the Menkes/Wilson disease proteins. *Nature Str. Biol.* **2000,** *7*, 766-771.

(93) Luczkowski, M.; Zeider, B. A.; Hinz, A. V. H.; Stachura, M.; Chakraborty, S.; Hemmingsen, L.; Huffman, D. L.; Pecoraro, V. L., Probing the coordination environment of the human copper chaperone HAH1: Characterization of Hg^{II}-bridged homodimeric species in solution. *Chem. Eur. J.* **2013,** *19*, 9042-9049.

(94) Lian, P.; Guo, H. B.; Riccardi, D.; Dong, A. P.; Parks, J. M.; Xu, Q.; Pai, E. F.; Miller, S. M.; Wei, D. Q.; Smith, J. C.; Guo, H., X-ray structure of a Hg^{2+} complex of mercuric reductase (MerA) and quantum mechanical/molecular mechanical study of Hg^{2+} transfer between the C-terminal and buried catalytic site cysteine pairs. *Biochemistry* **2014,** *53*, 7211-7222.

(95) Reed, A. E.; Curtiss, L. A.; Weinhold, F., Intermolecular interactions from a natural bond orbital, donor-acceptor viewpoint. *Chem. Rev.* **1988,** *88*, 899-926.

(96) Glendening, E. D.; Landis, C. R.; Weinhold, F., NBO 6.0: Natural bond orbital analysis program. *J. Comput. Chem.* **2013,** *34*, 1429-1437.

(97) Mehra, R. K.; Miclat, J.; Kodati, V. R.; Abdullah, R.; Hunter, T. C.; Mulchandani, P., Optical spectroscopic and reverse-phase HPLC analyses of Hg(II) binding to phytochelatins. *Biochem. J.* **1996,** *314*, 73-82.

(98) Krupp, E. M.; Mestrot, A.; Wielgus, J.; Meharg, A. A.; Feldmann, J., The molecular form of mercury in biota: identification of novel mercury peptide complexes in plants. *Chem. Comm.* **2009,** *28*, 4257-4259.

(99) Carrasco-Gil, S.; Alvarez-Fernandez, A.; Sobrino-Plata, J.; Millan, R.; Carpena-Ruiz, R. O.; Leduc, D. L.; Andrews, J. C.; Abadia, J.; Hernandez, L. E., Complexation of Hg with phytochelatins is important for plant Hg tolerance. *Plant Cell Environ.* **2011,** *34*, 778–791.

(100) Kawakami, S. K.; Achterberg, E. P., Particulate thiol peptides along a salinity gradient of a metal-contaminated estuary. *Estuar. Coast.* **2012,** *35*, 658-664.

(101) Dago, A.; Gonzalez, I.; Arino, C.; Martinez-Coronado, A.; Higueras, P.; Diaz-Cruz, J. M.; Esteban, M., Evaluation of mercury stress in plants from the Almaden mining district by analysis of phytochelatins and their Hg complexes. *Environ. Sci. Technol.* **2014,** *48*, 6256-6263.

(102) Steele, R. A.; Opella, S. J., Structures of the reduced and mercury-bound forms of MerP, the periplasmic protein from the bacterial mercury detoxification system. *Biochemistry* **1997,** *36*, 6885-6895.

(103) Rosenzweig, A. C.; Huffman, D. L.; Hou, M. Y.; Wernimont, A. K.; Pufahl, R. A.; O'Halloran, T. V., Crystal structure of the Atx1 metallochaperone protein at 1.02 angstrom resolution. *Structure* **1999,** *7*, 605-617.

(104) Banci, L.; Bertini, I.; Cantini, F.; Felli, I. C.; Gonnelli, L.; Hadjiliadis, N.; Pierattelli, R.; Rosato, A.; Voulgaris, P., The Atx1-Ccc2 complex is a metal-mediated protein-protein interaction. *Nature Chem. Biol.* **2006,** *2*, 367-368.

(105) Arnesano, F.; Banci, L.; Bertini, I.; Ciofi-Baffoni, S.; Molteni, E.; Huffman, D. L.; O'Halloran, T. V., Metallochaperones and metal-transporting ATPases: A comparative analysis of sequences and structures. *Genome Res.* **2002,** *12*, 255-271.

(106) Jalilehvand, F.; Leung, B. O.; Izadifard, M.; Damian, E., Mercury(II) cysteine complexes in alkaline aqueous solution. *Inorg. Chem.* **2006,** *45*, 66-73.

(107) George, G. N.; Pickering, I. J.; Prince, R. C.; Zhou, Z. H.; Adams, M. W. W., X-ray absorption spectroscopy of *Pyrococcus furiosus* rubredoxin. *J. Biol. Inorg. Chem.* **1996,** *1*, 226-230.

(108) Faller, P.; Ctortecka, B.; Troger, W.; Butz, T.; Vasak, M., Optical and TDPAC spectroscopy of Hg(II)-rubredoxin: model for a mononuclear tetrahedral $Hg(CysS)_4^{2-}$ center. *J. Biol. Inorg. Chem.* **2000,** *5*, 393-401.

(109) Maher, M.; Cross, M.; Wilce, M. C. J.; Guss, J. M.; Wedd, A. G., Metal-substituted derivatives of the rubredoxin from *Clostridium pasteurianum*. *Acta Cryst. D.* **2004,** *60*, 298-303.

(110) Utschig, L. M.; Bryson, J. W.; O'Halloran, T. V., Mercury-199 NMR of the metal receptor site in MerR and its protein-DNA complex. *Science* **1995,** *268*, 380-385.

(111) Alsina, T.; Clegg, W.; Fraser, K. A.; Sola, J., Homoleptic cyclohexanethiolato complexes of mercury(II). *J. Chem. Soc. Dalton Trans.* **1992,** *8*, 1393-1399.

(112) Stillman, M. J., Metallothioneins. *Coord. Chem. Rev.* **1995,** *144*, 461-511.

(113) Rodic, D.; Spasojevic, V.; Bajorek, A.; Onnerud, P., Similarity of structure properties of $Hg_{1-x}Mn_xS$ and $Cd_{1-x}Mn_xS$ (structure properties of HgMnS and CdMnS). *J. Mag. Mag. Mater.* **1996,** *152*, 159-164.

(114) Thomas, S. A.; Gaillard, J. F., Cysteine addition promotes sulfide production and four-fold Hg(II)-S coordination in actively metabolizing *Escherichia coli*. *Environ. Sci. Technol.* **2017,** *51*, 4642-4651.

(115) Thomas, S. A.; Rodby, K. E.; Roth, E. W.; Wu, J.; Gaillard, J. F., Spectroscopic and microscopic evidence of biomediated HgS species formation from Hg(II)–cysteine complexes: Implications for Hg(II) bioavailability. *Environ. Sci. Technol.* **2018,** *52*, 10030-10039.

(116) Fowle, D. A.; Stillman, M. J., Comparison of the structures of the metal-thiolate binding site in Zn(II)-, Cd(II)-, and Hg(II)-metallothioneins using molecular modeling techniques. *J. Biomol. Str. Dyn.* **1997,** *14*, 393-406.

(117) Demchenko, I. N.; Denlinger, J. D.; Chernyshova, M.; Yu, K. M.; Speaks, D. T.; Olalde-Velasco, P.; Hemmers, O.; Walukiewicz, W.; Derkachova, A.; Lawniczak-Jablonska, K., Full multiple scattering analysis of XANES at the Cd L_3 and O *K* edges in CdO films combined with a soft-x-ray emission investigation. *Phys. Rev. B* **2010,** *82*, 075107.

(118) Ankudinov, A. L.; Rehr, J. J.; Low, J. J.; Bare, S. R., Sensitivity of Pt x-ray absorption near edge structure to the morphology of small Pt clusters. *J. Chem. Phys.* **2002,** *116*, 1911-1919.

(119) Glendening, E. D.; Landis, C. R.; Weinhold, F., NBO 6.0: Natural bond orbital analysis program. *J. Comput. Chem.* **2013,** *34*, 1429-1437

LEGENDS TO FIGURES

Figure 1. (a) Mercury L_3-edge HR-XANES spectra of the initial aged Hg-DOM (28 μg Hg/g DOM_i, purple) and the final Hg-DOM from aquaria with fish after eight weeks (2 μg Hg/g DOM_f, blue). (b) Comparison of the final Hg-DOM spectrum with spectra from Hg linearly complexed to thiol ligands from the humic acid fraction of the DOM ($Hg(SR)_2$ complex[36]) (green) and from nanoparticulate β-HgS (metacinnabar) (black). The $Hg(SR)_2$ reference was obtained by reacting $Hg(NO_3)_2$ with the *Carex* peat HA isolate for 15 h to minimize formation of nanoparticulate β-HgS[37], and β-HgS_{NP} was synthesized at room temperature (RT) from Hg-(L-Cys-OEt)$_2$ complex aged for 80 days in contact with air.[37] The increase in proportion of $Hg(SR)_2$ is detected in plots (a) and (b) by an increase of the near-edge peak at 12279.5 eV, a direct indicator of Hg(II) linearly coordinated to two thiol ligands,[36, 37] and a shift to higher energy of the trailing edge of the spectrum (arrows in (a)). Tetrahedral bonding of mercury to four sulfur atoms in β-HgS_{NP} is seen as a shoulder instead of a peak on the rising part of the spectrum. (c) Linear least-squares fit (orange) to the Hg-DOM_f spectrum (blue) with 63 ± 10% $Hg(SR)_2$ and 37 ± 10% nanoparticulate β-HgS. The normalized sum-squared residual (*NSS*) is the normalized difference between two spectra expressed as $\Sigma[(y_{exp}-y_{fit})^2]/\Sigma(y_{exp}^2)$. Top, ball-and-stick representation of the Hg-thiolate complex and polyhedral representation of the β-HgS structure.

Figure 2. (a) Mercury L_3-edge HR-XANES spectrum of fish (Fish-DOM) exposed to Hg-DOM_i = 1453 μg Hg/g with spectra from the initial and final DOMs. (b) HR-XANES spectra of fish exposed

793 to DOM_i-1453, dietary MeHg, and $HgCl_2$ (8 μg/L). The Fish-MeHg spectrum has an intense near-
794 edge peak at 12279.8 eV and the Fish-Hg spectrum has a weak peak, more like β-HgS_{NP} (Figure
795 1b). (c) Linear least-squares fit (orange) to the Fish-DOM spectrum (green) with a mixture of the
796 Fish-MeHg and Fish-Hg spectra shows that Hg has a unique chemical form in the fish exposed to
797 the Hg-DOM.
798
799 **Figure 3.** Mercury coordination in fish contaminated by Hg-DOM (DOM_i-1453) derived from Hg
800 L_3-edge HR-XANES. (a) A one-component fit to all reference spectra identified the dithiolate
801 complexes $Hg(GSH)_2$ and ($Hg(Cys)_2$) at physiological pH as the closest model compounds to the
802 binding environment of Hg in fish ($Hg[(SR)_2+(N/O)_{1-2}]$ coordination, Figures 4a and S9). (b) A
803 two-component fit further identified the tetrathiolate complex $Hg(Cys)_4$ as secondary model
804 species. (c) Fitting residuals were used to evaluate the magnitude of the resultant uncertainty of
805 the determined Hg coordinations. The residual of the $Hg(Cys)_2$ + $Hg(Cys)_4$ reconstruction is close
806 to experimental noise and has a smaller NSS value than the $Hg(GSH)_2$ + $Hg(Cys)_4$ reconstruction
807 (1.06×10^{-4} vs 1.28×10^{-4}).
808
809 **Figure 4.** (a) Geometry-optimized model of the molecular structure of the $Hg(GSH)_2$ complex
810 (Video S1). Hg(II) is bridged to two primary SR^- thiolate ligands (one from each GSH molecule)
811 and two secondary O ligands from the same GSH molecule forming an intramolecular double-ring
812 chelate. The $Hg(GSH)_2$ complex is further stabilized by an extended intermolecular H-bond
813 network involving the protonated amino groups ($-NH_3^+$) and deprotonated carboxyl groups of the
814 two glutamate residues. The two H-bridged peptides form a molecular scaffold which binds Hg(II)
815 in a pseudo claw-setting environment. (b) Geometry-optimized $Hg_3(SMe)_9$ and $Hg_4(SMe)_{11}$
816 clusters featuring the inorganic core structure of the Hg-β and Hg-α domains in vertebrate
817 metallothionein. (c) $\{Hg_3S_9\}$ and $\{Hg_4S_{10}\}$[95, 119] motifs of the β-HgS structure[113] showing the
818 similarity of the polyhedral associations with the metallothionein clusters. See Ref.[48] for details.
819 MP2/TZVP-ecp optimization. Bond lengths, in angstroms, and bond angles are in black. Atomic
820 charges, in units of elementary charge e and calculated by natural population analysis (NPA[95, 119]),
821 are in blue. Dark red, Hg; yellow, S; blue, N; red, O; gray, C; light gray, H. Cartesian coordinates of
822 the $Hg(GSH)_2$ model are provided in the SI.
823

TABLE 1. Samples codes and concentration of Hg in the initial and final Hg(II)-spiked DOM and in fish

Experiment[a]	Initial Hg[b] [µg/g DOM]	Initial Hg[c] in water [µg/L]	Final Hg[b] [µg/g DOM]	Final DOM sample code	[Hg] in water (µg/L) at t_8	Whole fish Hg[d] [µg/g] at t_8	Fraction of Hg in fish at t_8 [%][e]
DOM_i-28	28 ± 3	3 ± 6	2 ± 1	DOM_f-2	1.3 ± 0.3	0.33 ± 0.03	1.9 ± 0.4
DOM_i-270	270 ± 3	31 ± 5	27 ± 1	DOM_f-27	11.5 ± 0.5	1.06 ± 0.08	0.88 ± 0.07
DOM_i-1453	1453 ± 8	124 ± 6	240 ± 1	DOM_f-240	70 ± 2.8	2.20 ± 0.14	0.32 ± 0.02
$HgCl_2$ (C_{Hg})		5.2 ± 0.6			1.1 ± 0.2	10.4 ± 0.3	50 ± 9

[a]Values represent averages from duplicate experimental aquaria. [b]Concentrations measured on freeze-dried DOM. [c]Concentration of Hg in unfiltered water. [d]Concentration based on dry weight. [e]Calculation performed by dividing the total amount of accumulated Hg in whole fish by the total amount of Hg present in the aquaria (35 L), both at t_8. The first quantity was obtained by multiplying the total number of fish at t_8 (n = 46) by the corrected concentration of Hg in whole fish at t_8 and the average dry fish weight of 80.5 ± 20 mg. The corrected concentration of Hg in whole fish at t_8 is the concentration accumulated between t_0 and t_8 and therefore calculated by subtracting from the whole fish Hg concentration at t_8 that of control fish at t_0 equal to 0.09 ± 0.03 µg/g dry weight.

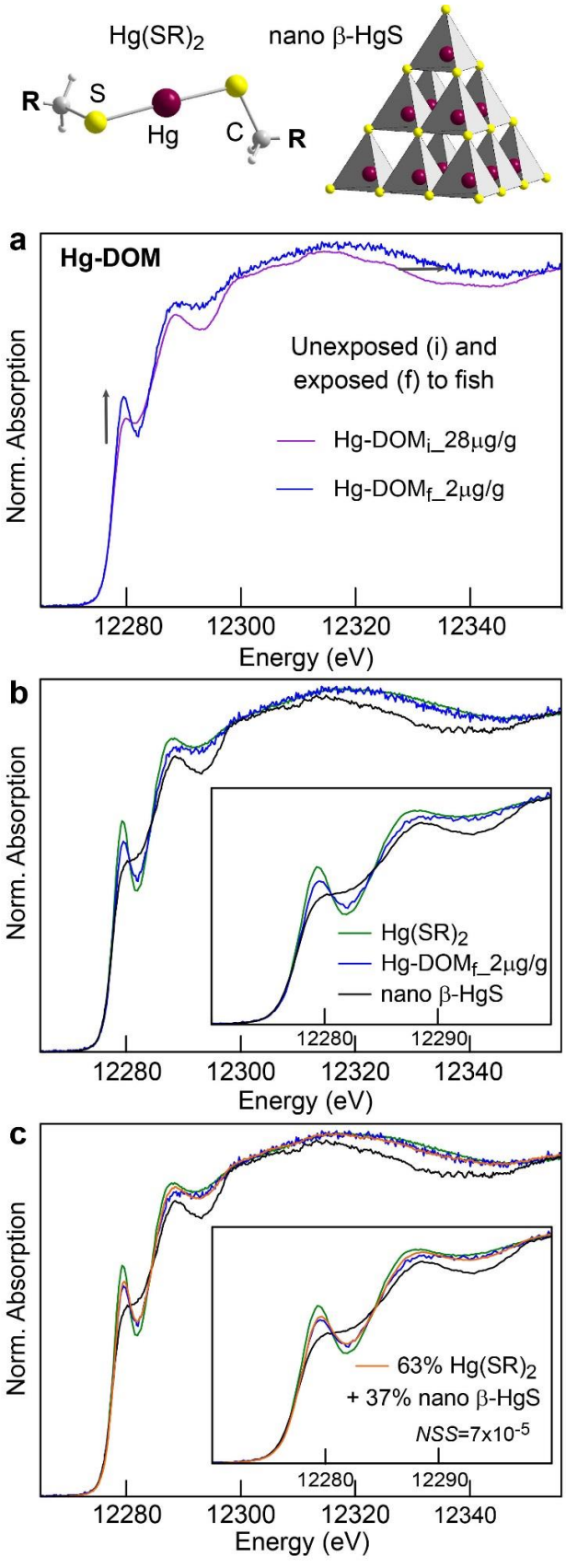

Figure 1

Please, print to fit the full width of one column, thank you

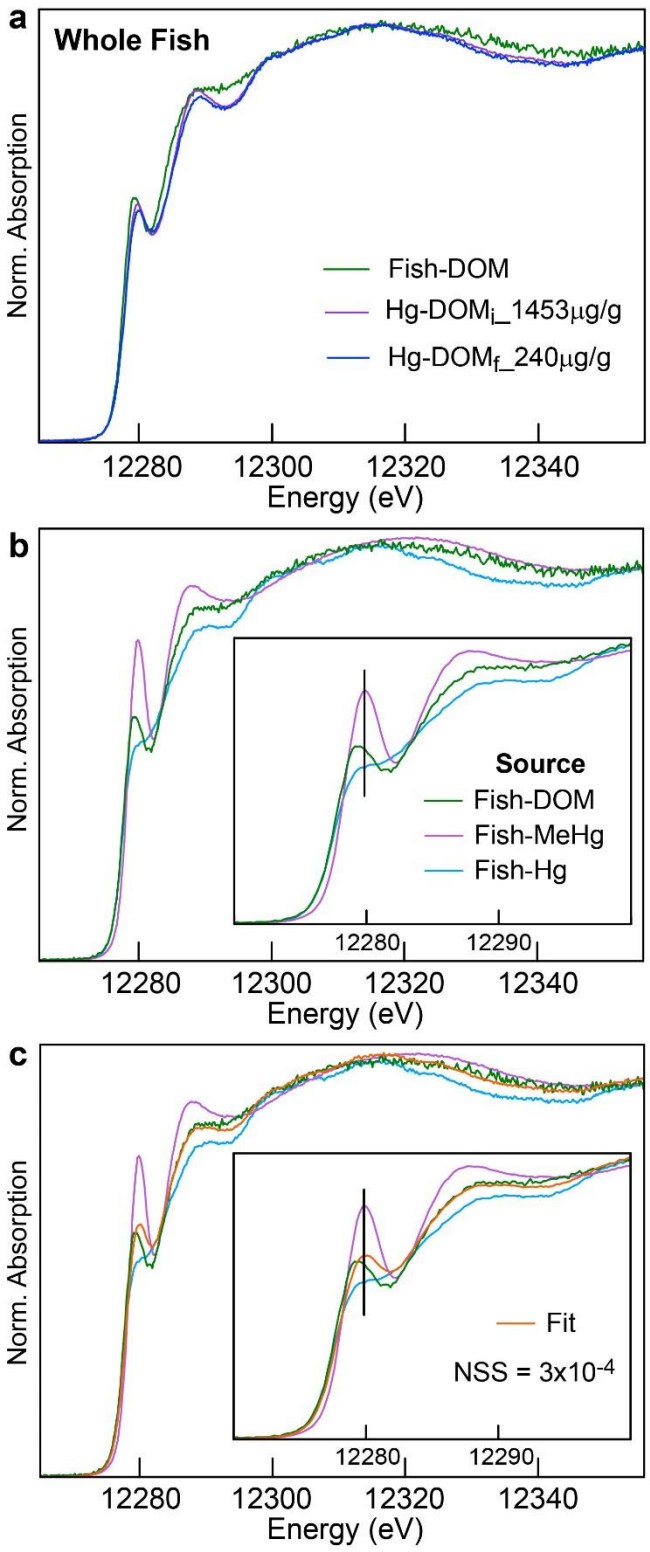

Figure 2

Please, print to fit the full width of one column, thank you

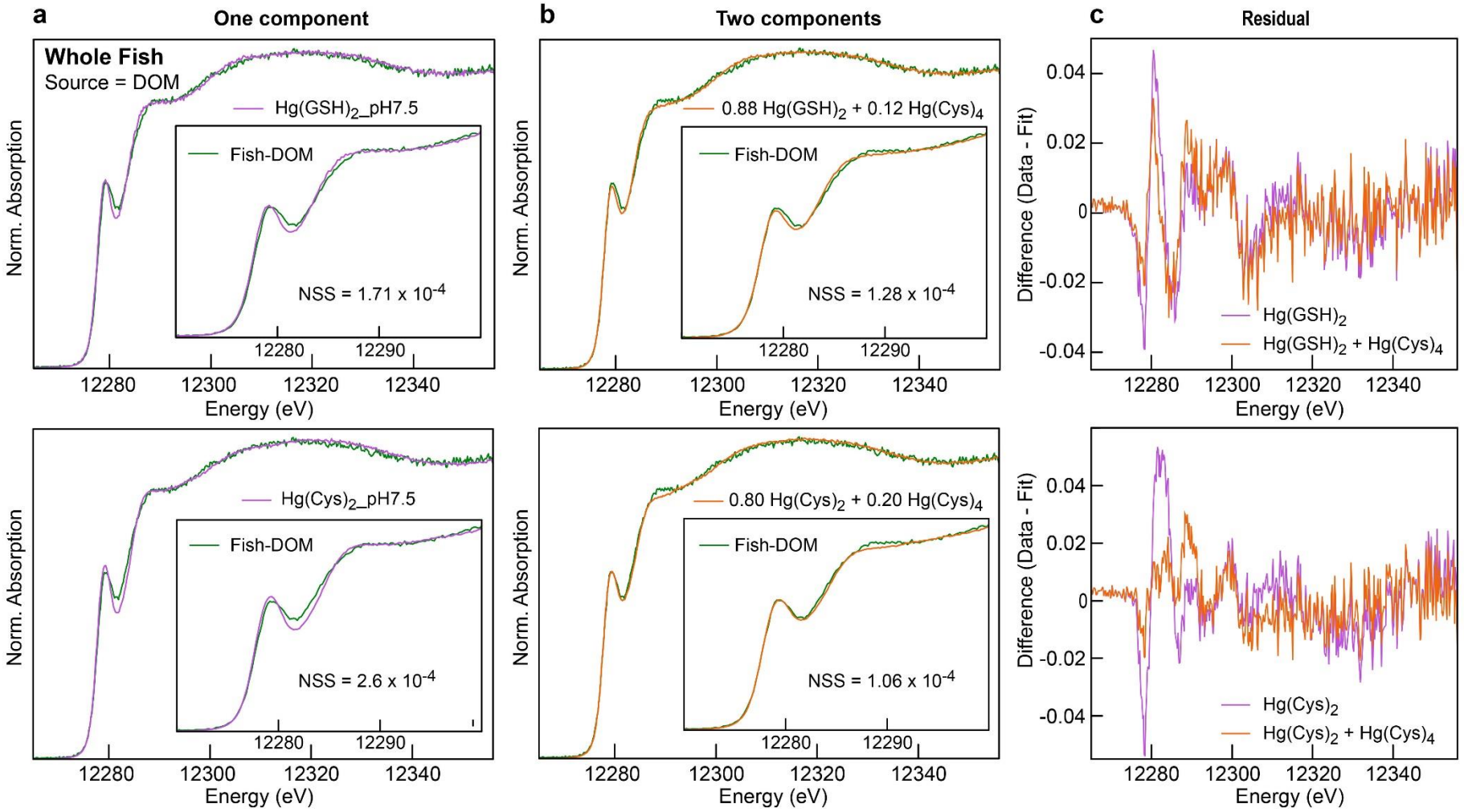

Figure 3

Please, print to fit the full width of two columns, thank you

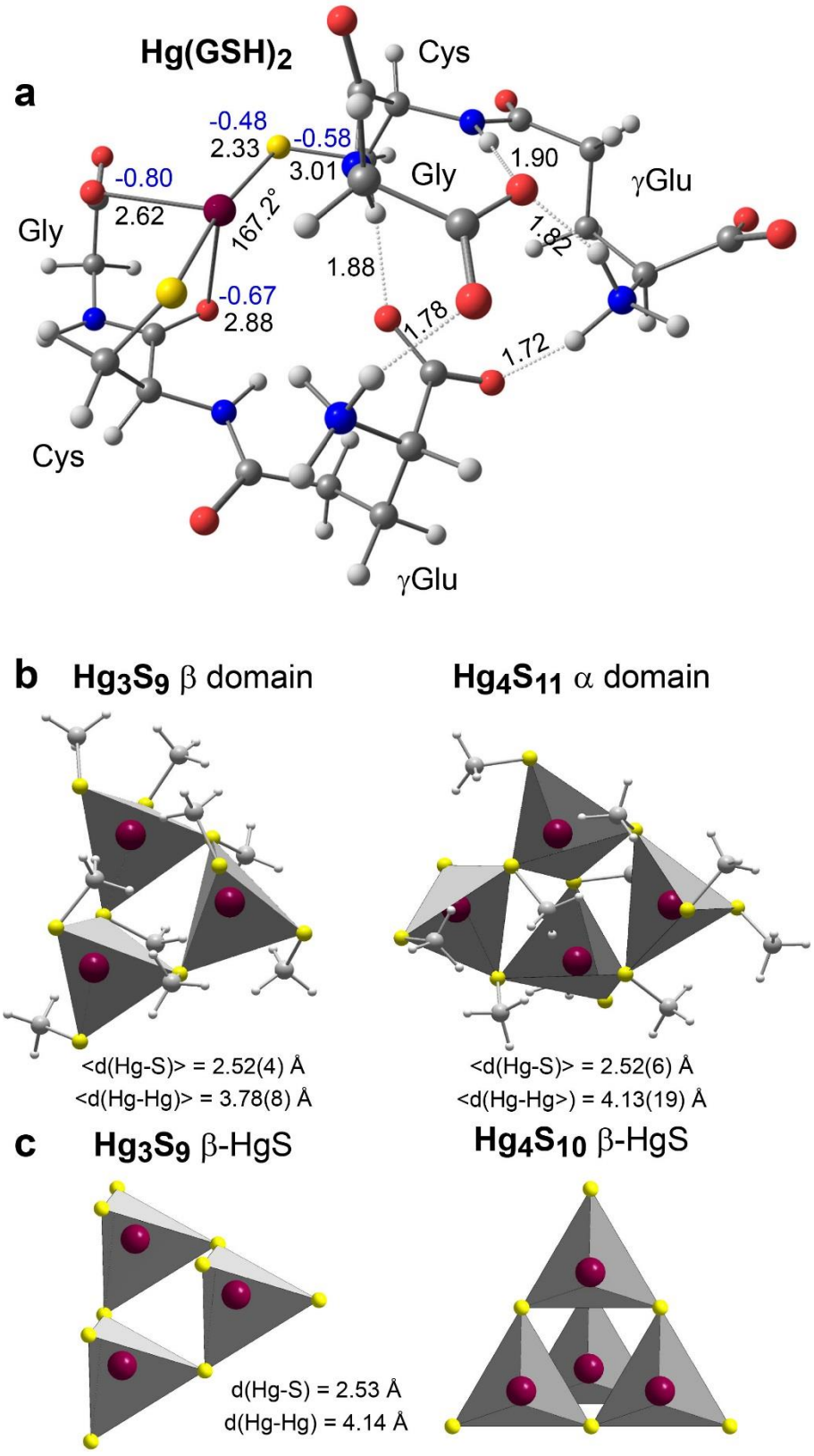

Figure 4

Please, print to fit the full width of one column, thank you